Clean Technologies and Recycling

Clean Technologies and Recycling, 1(2): 124–151.
DOI: 10.3934/ctr.2021007
Received: 09 June 2021
Accepted: 25 October 2021
Published: 03 November 2021

http://www.aimspress.com/journal/ctr

Review

Direct recycling technologies of cathode in spent lithium-ion batteries

Yi Ji[1], Edwin E. Kpodzro[2,3], Chad T. Jafvert[4] and Fu Zhao[1,2,*]

[1] Environmental and Ecological Engineering, Purdue University, West Lafayette, IN 47907, USA
[2] Mechanical Engineering, Purdue University, West Lafayette, IN 47907, USA
[3] Ecological Sciences and Engineering, Purdue University, West Lafayette, IN 47907, USA
[4] Lyles School of Civil Engineering, Purdue University, West Lafayette, IN 47907, USA

* **Correspondence:** Email: fzhao@purdue.edu.

Abstract: Lithium-ion battery (LIB)-based electric vehicles (EVs) are regarded as a critical technology for the decarbonization of transportation. The rising demand for EVs has triggered concerns on the supply risks of lithium and some transition metals such as cobalt and nickel needed for cathode manufacturing. There are also concerns about environmental damage from current recycling and disposal practices, as several spent LIBs are reaching the end of their life in the next few decades. Proper LIB end-of-life management can alleviate supply risks of critical materials while minimizing environmental pollution. Direct recycling, which aims at recovering active materials in the cathode and chemically upgrading said materials for new cathode manufacturing, is promising. Compared with pyrometallurgical and hydrometallurgical recycling, direct recycling has closed the material loop in cathode manufacturing via a shorter pathway and attracted attention over the past few years due to its economic and environmental competitiveness. This paper reviews current direct recycling technologies for the cathode, which is considered as the material with the highest economic value in LIBs. We structure this review in line with the direct recycling process sequence: cathode material collection, separation of cathode active materials from other components, and regeneration of degraded cathode active materials. Methods to harvest cathode active materials are well studied. Efforts are required to minimize fluoride emissions during complete separation of cathode active materials from binders and carbon. Regeneration for homogeneous cathode is achieved via solid-state or hydrothermal re-lithiation. However, the challenge of how to process different cathode chemistries together in direct recycling needs to be solved. Overall, the

development of direct recycling provides the possibility to accelerate the sustainable recycling of spent LIBs from electric vehicles.

Keywords: lithium-ion batteries; direct recycling; end-of-life; cathode

Abbreviations: CAMs: Cathode active materials; DMAC: N,N-dimethylacetamide; DMF: N,N-dimethylformamide; DMSO: N,N-dimethyl sulfoxide; EVs: Electric vehicles; LCO: $LiCoO_2$; LFP: $LiFePO_4$; LIBs: Lithium-ion batteries; LMO: $LiMn_2O_4$; NCA: $LiNiCoAlO_2$; NMC: $LiNi_xMn_yCo_zO_2$; NMP: N-Methyl-2-pyrrolidone; PVDF: Polyvinylidene fluoride.

Others:
Battery cells: Here only pouch cells used in electric vehicles are considered. They are composed of casing/pouch, a series of electrode (anode/cathode) sheets, separators, and electrolytes.
Anode/cathode sheets: They are composed of current collect (Cu/Al foil) and two anode/cathode layers.
Cathode layer/cathode materials: Materials are coated on current collectors (Al foils). They are composed of cathode active materials (metal oxides), conductive materials (i.e. acetylene black), and binders.
Anode layer/anode materials: Materials are coated on current collectors (Cu foils). They are composed of anode active materials (i.e. graphite) and binders.

1. Introduction

Lithium-ion batteries (LIBs) are widely used in electronic devices such as cell phones, laptops, cameras, electric vehicles (EVs) and others because of their high energy density, stability, and affordability [1]. In the next few decades, the demand for EVs brings a new challenge to CAMs supply [2]. The number of EVs on the road worldwide is projected to rise to 140 million by 2030 [3]. The production of EVs will increase 2–3 times from 2025 to 2050 [4]. In addition, the supply risks of lithium and transition metals used in cathode active materials (CAMs) are widely recognized [5]. It is predicted that between 0.33 million to 4 billion LIBs are expected to reach the end of their service lives between 2015 and 2040 [6]. Recycling end-of-life EV LIBs can alleviate the supply risks of critical materials. However, depending on technologies used, LIBs recycling may result in water pollution from leachate, solid waste such as metal-rich ash, and air pollution [7]. There is a critical need to developing economically viable and environmentally friendly recycling technologies for spent EV LIBs (especially the cathodes).

The structure of LIBs used in EVs is shown in Figure 1. Inside the battery casing, there are a series of electrodes (anode sheets and cathode sheets) with separators and electrolytes. The separators are made of polymers, e.g., polypropylene or polyethylene, which allow active lithium ions to transfer during charging and discharging [8]. The lithium salt electrolyte, e.g., $LiPF_6$, $LiClO_4$, and $LiBF_4$, and cyclic or linear carbonate solvents (ethylene carbonate) are injected into battery cells [9,10]. Copper foils are used as anode current collectors, and aluminum foils are used as

cathode current collectors [11]. The anode layer, which stores active lithium ions after charging, has graphite as the active material with polyvinylidene fluoride (PVDF) as the binder [12]. A typical cathode layer includes 80–85% cathode active materials (CAMs), ~10% PVDF binder, and ~5% acetylene black conductive materials [7]. The chemistries of CAMs include, but are not limited to, $LiFePO_4$ (LFP), $LiCoO_2$ (LCO), $LiMn_2O_4$ (LMO), and $LiNi_xMn_yCo_zO_2$ (x = y = z = 0.333, NMC111; x = 0.5, y = 0.3, z = 0.2, NMC523; x = 0.6, y = z = 0.2, NMC622; x = 0.8, y = z = 0.1, NMC811) [13]. In commercial LIB cathode production, the PVDF binder is pre-dissolved in solvent; N-Methyl-2-pyrrolidone (NMP) is commonly used [14,15]. Then, the PVDF binder with NMP is uniformly mixed with CAMs and acetylene black to form slurry. The final slurry is cast onto the Al foils (cathode current collectors) and dried at 120°C for 12–24 hours to evaporate the NMP solvent [16].

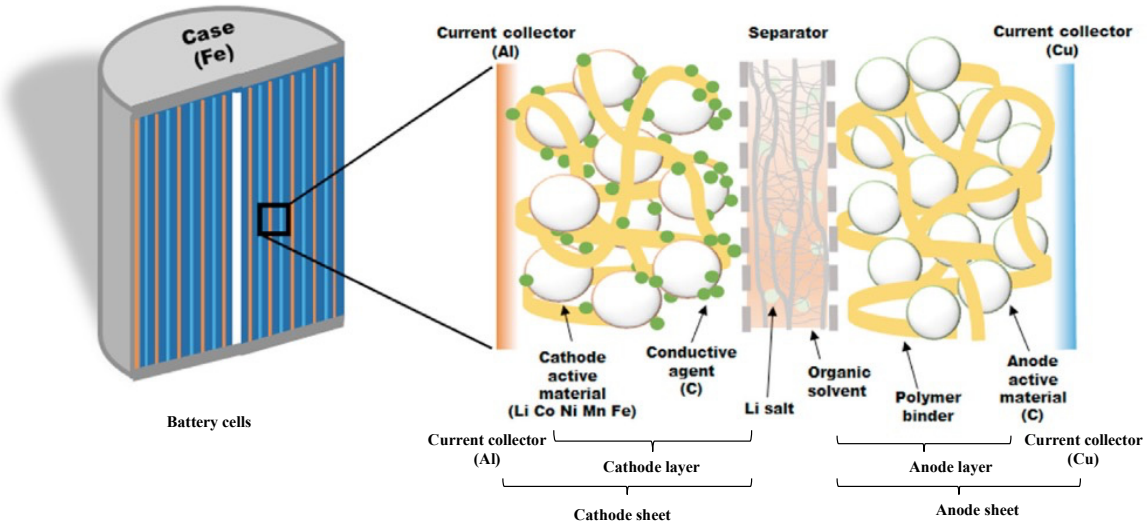

Figure 1. A schematic diagram of the lithium-ion batteries components. Figure adapted from Kim et al. [17].

Current approaches to the recycling of spent LIBs can be classified into pyrometallurgical, hydrometallurgical, and direct recycling as shown in Figure 2 [18]. Pyrometallurgical recycling requires high temperatures to reduce cathode to an alloy of transition metals, which results in high energy consumption and air emission [19]. The reaction temperature is about 1000°C to form Co-, Fe-, and Ni- based alloys [19]. The gas products released at lower temperatures contain decomposition products from binders and electrolyte [20]. The advantage of the pyrometallurgical method is that it can handle a large number of spent LIBs without pretreatment processes. Leaching, bioleaching, and solvent extraction are key methods of hydrometallurgical recycling [21]. Valuable metals are recovered in solution and resynthesized to metal oxides, relying on complex operation steps. Compared with pyrometallurgical technologies, hydrometallurgical technologies achieve high selectivity and high recycling efficiency, and produce value-added products [21,22]. The removal of cathode/anode active materials and their reuse in remanufactured LIBs is known as direct recycling [23]. For many cathode chemistries including lithium nickel manganese cobalt oxide

(NMC622), lithium nickel cobalt aluminum oxide (NCA), and lithium iron phosphate (LFP), direct recycling has a higher recovery rate of CAMs while employing simpler processes, compared with pyrometallurgical and hydrometallurgical recycling; this leads to greater environmental and economic benefits [24].

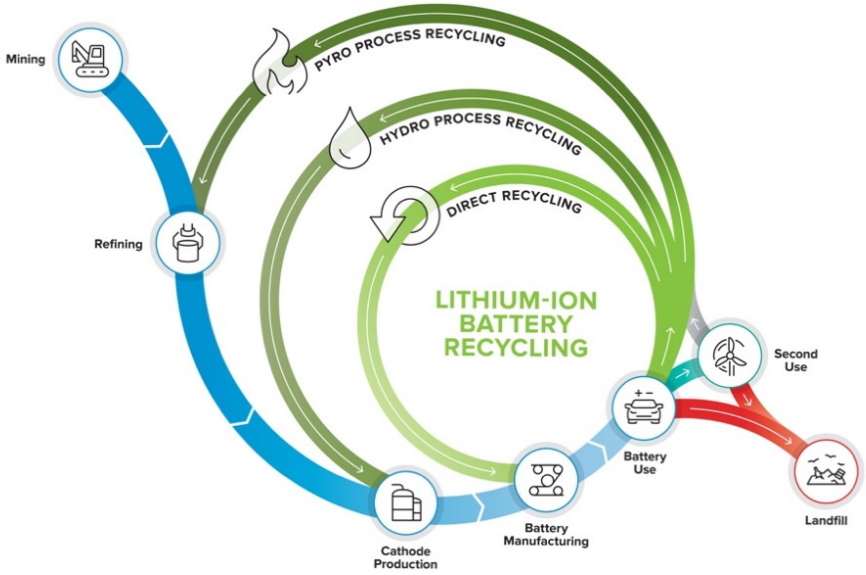

Figure 2. Life Cycle of a Lithium-Ion Battery [18].

The typical direct recycling processes are summarized in Figure 3. In general, the direct recycling process for cathodes involves three steps. The first step is to harvest cathode materials (Section 2 and 3). If battery cells are directly crushed (Section 2), a separation process must be undertaken to separate metal-containing components from polymers in the ensuing mixture of metals (casing), anode/cathode materials, and separators (polymers). Whether cathodes and anodes are crushed together or only cathodes are crushed, cathode materials must be separated from current collectors. To avoid contamination from current collectors, researchers focus on separating the cathode layer from the cathode sheet after manual/mechanical dismantlement in order to collect cathode materials (Section 3). Relevant methods mainly involve three mechanisms: dissolution of PVDF, decomposition of PVDF, and dissolution of Al foil. The second step is the separation of CAMs from PVDF/carbon (Section 4). The commonly used approach includes thermal treatment and flotation. The final step is to regenerate the degraded electrochemical performance of CAMs from spent LIBs (Section 5). The current cathode chemistries of spent LIBs include LCO, LFP, LMO, and NCA from generation 1 batteries; NMC111 and NMC523 from generation 2 batteries; NMC622, and NMC811 from generation 3 batteries [23]. The recycled CAMs from direct recycling should have the same cathode chemistries as before. After regeneration, the recycled CAMs can be used to manufacture new cathodes/cells. This paper reviews recent developments in technologies related to direct cathode recycling. Advantages and disadvantages of these technologies are discussed, and further research needs are suggested.

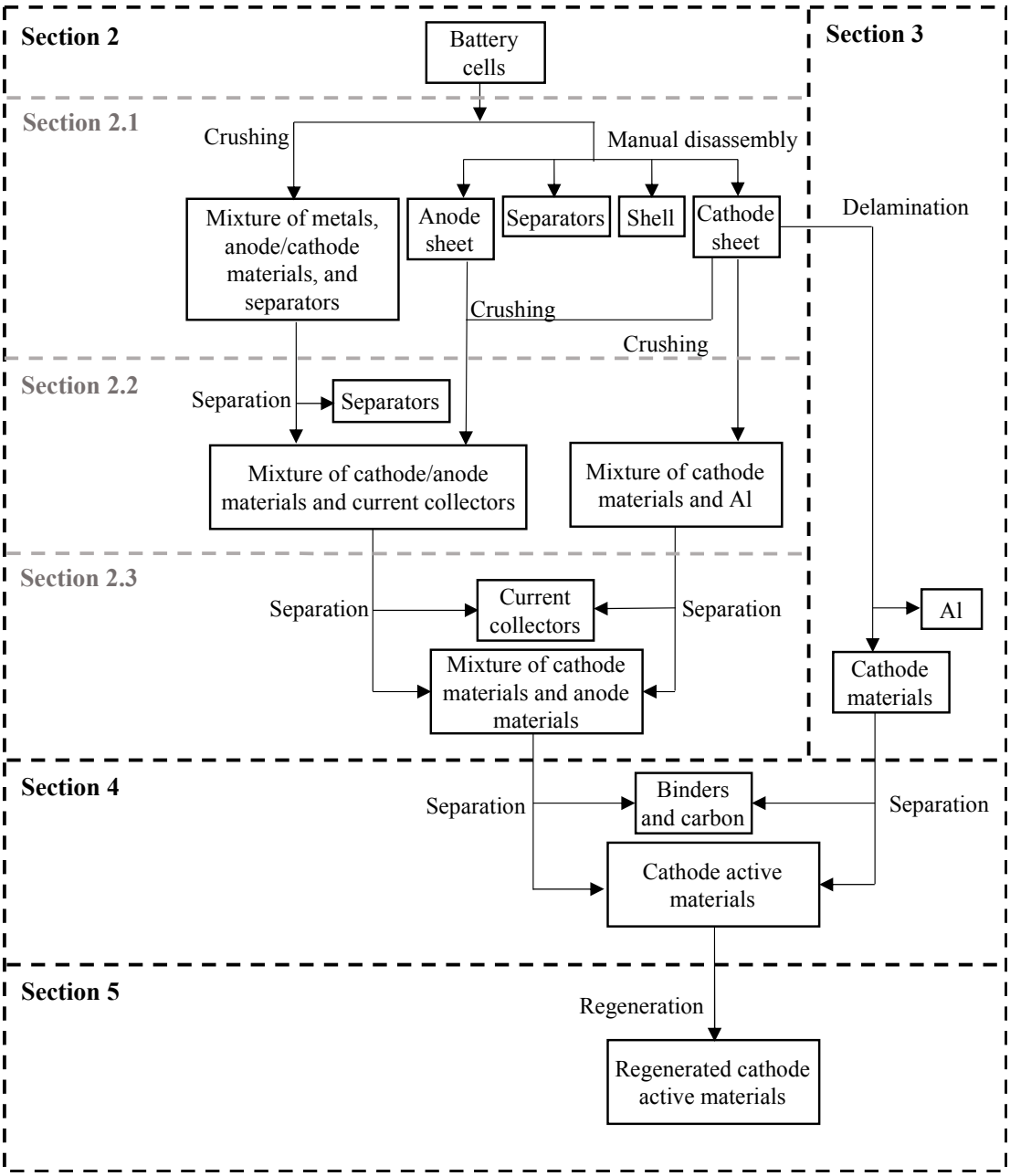

Figure 3. Flow diagram for direct recycling processes of cathodes.

2. Cathode materials collection after crushing

Rotating comminution processes are considered as important methods to minimize the particle size of components in spent LIBs [25]. Rotating comminution processes are illustrated in Section 2.1. If pouch cells are directly crushed, the resulting mixture includes metals (casing and cathode/anode current collectors), anode/cathode materials, and separators (polymers). If cathode and anode sheets from manual dismantlement are crushed, the resulting mixture contains cathode/anode materials and current collectors (Cu and Al). Crushing of cathode sheets leads to a mixture of cathode materials and Al.

Because various mixtures are obtained depending on pretreatment processes, the different approaches are summarized in terms of removed components. The removal of polymers is illustrated in Section 2.2. The separation of current collectors from cathode materials is discussed in Section 2.3. In this section (Section 2), we focus on processes to obtain cathode materials after comminution processes. Besides crushing cathode sheets, methods for the removal of cathode materials from the Al current collector (delamination) are discussed in the next section (Section 3).

2.1. Comminution of battery cells or electrodes

2.1.1. Comminution of battery cells

Direct crushing of pouch cells avoids the need for manual disassembly of different components. Thus, this process is more feasible in large-scale operation. Wet crushing and dry crushing are compared for LCO pouch cells [26]. The wet crushing process uses a blade crusher operating at high speed with water as the medium. The dry crushing includes two stages: (1) spent LIB pouch cells are cut into small pieces by a shear crusher and (2) the small pieces are crushed by an impact crusher for 20 s. For both approaches, the coarse size fraction (>2 mm) and fine size fraction (<0.075 mm) are large, and medium size fraction (~0.075–2 mm) is small. In wet crushing, the cathode layer cannot be easily liberated from Al foil and is not easily transferable through mesh due to the presence of water. The composition in fine size fraction is complex (includes CAMs, C, Cu, and Al). The CAMs are removed with water, leading to a reduction in material quantity. On the contrary, in dry crushing, particle size less than 0.075 mm is mainly composed of graphite. Details about dry crushing are provided by the same authors in another study. Al is enriched in particle size above 2 mm, and $LiCoO_2$ and graphite are enriched in particle size below 0.25 mm [27]. The recovery rate of Co fraction (<0.25 mm) is 94.29%. Impurities include, but are not limited to, Cu, Al, F, Mn, P, Cl, Zn, and Fe. Cl and Zn contaminants are introduced from grinding instruments. In addition, the wet crushing process is used by Barik et al [28]. The battery cells are fed into a shredder with water as a scrubbing agent. The recycled particle size is less than 10 mm. The polymers that float on the water are manually taken out. The recycled mixture contains CAMs, Cu foils, Al foils/casings, PVDF, and carbon. Therefore, dry crushing is recommended since wet crushing leads to mass loss and introduces more Al. It is noted that LCO cathode materials concentrate in fine fraction. Crushing and screening multiple times may minimize impurities in recycled cathode materials.

The two-step crushing of battery cells is proposed to increase the recovery rate of cathode and anode coating for NMC-based LIBs [29]. In addition, the influences of second crushing are studied. The first step employs a six-disk-rotor cutting mill under nitrogen atmosphere to recover heavy parts >20 mm, e.g., casing materials, electric conductors, and steels screws. The released gases contain electrolyte solvents and carbon dioxide. This result highlights the importance of gas collection or treatment in direct recycling. The second step employs a cutting mill followed by screening (10 mm) and air-classification. With second crushing, the yield of black mass (NMC and graphite) increases from 60% to 75%. The percentages of impurities of Al, Cu, and Fe are hardly changed with or without second crushing.

2.1.2. Comminution of cathodes and anodes

To avoid polymer and casing contamination, cathodes and anodes are crushed together after manual disassembly. The subsequent separation of Cu/Al from cathode materials is necessary. The influence of grinding time on subsequent separation are studied [30]. First, cathode strips and anode strips are mixed in the impact crusher (cathode to anode ratio of 1:1) to reduce the particle size (<0.074 mm). Then, the mixed electrode powder is ground by steel balls in a sealed grinding chamber. The grinding time is set from 2.5 min to 30 min. The dry modification mechanism is proposed to explain how the grinding time affects the subsequent flotation separation (Figure 4). The steel balls provide both horizontal shear force and vertical rolling pressure. The horizontal shear force enlarges the hydrophobic surface of graphite because of the sliding and flaking movement of graphite, and enlarges hydrophilicity of $LiCoO_2$ by smoothening the protrusions and removing the organic film coating on LCO surface. The vertical rolling pressure tends to promote the aggregation of graphite and LCO. The optimal grinding time is 5 minutes when graphite and LCO have balanced hydrophobicity/hydrophilicity and particle size to separate. After long grinding time, small hydrophobic graphite particles are adsorbed on hydrophilic $LiCoO_2$ particles forming agglomerates. This results in separation difficulties of CAMs and graphite.

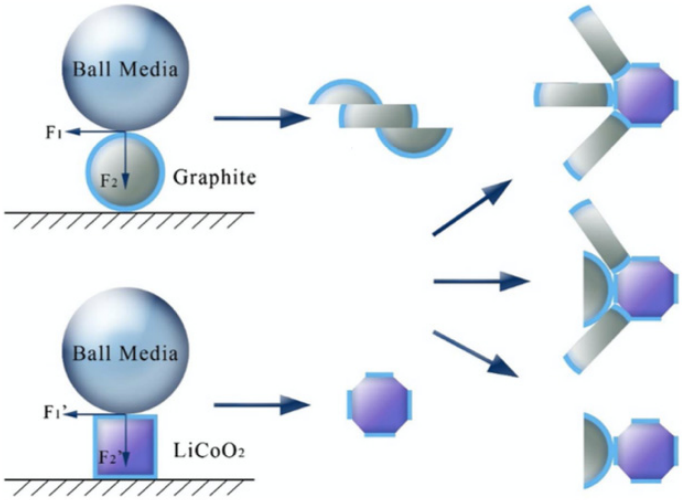

Figure 4. Dry modification mechanism based on mechanical abrasion [30].

2.1.3. Comminution of cathodes

The complex compositions result in subsequent separation difficulties, and thus, crushing only the cathode sheets rather than the entire battery cells or cathode and anode sheets together is more desirable in direct recycling. A planetary ball mill is used to grind cathodes after manual dismantlement of battery cells in laboratory scale. This approach is commonly used as pre-treatment to minimize leaching time before hydrometallurgical recycling [31,32]. The labor cost is not negligible to separate anodes, separators, and metal shells. If cathodes are harvested, delamination of cathode materials from cathodes is another approach to avoid Al contamination (Section 3).

2.2. Separation of metal-containing components from polymers

If battery cells are crushed, the separators are first removed because of their significant characteristic differences from other components. The electrostatic separation is based on the electrical property differences of LIB components. The polymers are nonconductive materials whereas metals (Cu, Al, and steel) are conductive. After drying to remove electrolyte and screening to remove LCO, the roll-type electrostatic divider could recover 99.6% of polymers and 98.98% of metals (the mixture of Cu, Al, and steel) [33]. The divider is composed of two parts: ionization electrodes and static electrodes. The ionization electrodes pin the nonconductive materials onto the rolls, which are collected at the end of rolls, and static electrodes attract conductive materials. Those that are not classified as conductors or nonconductors, are considered as middlings. The optimized conditions are electrode voltage, roll rotation speed, distance of the electrostatic electrode, and the inclination angle of the deflector. Widijatmoko et al. apply and modify this process [34]. Deflector angle is added as another parameter. The 2.5 min attrition scrubbing is added to liberate cathode materials from current collector, and the iron silica sand (2360–850 um) is used as the attrition medium. The wet sieving is used after electrostatic separation, and 80% LCO is recycled with impurities of 7% Al and 6.1% Cu in the size fraction of <38 um. The attrition medium is not strongly pinned by ionization electrodes or strongly attracted by static electrodes. Additive iron silica sand affects the impurity of recycled cathode materials, while 99% can be recycled in middlings with polymers in the size fraction of <850 um. The middling, which contains little Al and Cu after one electrostatic separation, is reintroduced for five repetitions. Reintroduction makes the process more complicated.

The polymers can be easily removed from the mixture because of their low density. The density separation is used to recycle Cu and polyethylene separators [35]. The density of Cu and polyethylene are 8.96 g/cm^3 and 0.9 g/cm^3, respectively. The mixture is put into diiodomethane solution (density of 3.3 g/cm^3), and the floats and sediments are separated in 30 minutes. A commercial scale Recupyl process applies density separation after screening and magnetic separation (to move steel components), plastic, paper, Al foil, and Cu foil are separated by densimetric tables [36].

Pneumatic separation is considered as a simple, low cost, and reliable approach to achieve solid-solid separation according to density differences of metallic and non-metallic materials [37]. Huang et al. study air separation in a zigzag classifier although the performance is not ideal [38]. The air velocity in the zigzag channel is 1.5–4.5 m/s. The products are classified into four fractions based on particle size: <0.5 mm, 0.5–1 mm, 1–2 mm, and >2 mm. The non-metallic fractions are 32.4 wt%, 23.4 wt%, 27.4 wt%, and 5.8 wt%, respectively. It is noted that a considerable number of polymers are mixed with cathode materials in small particle size (<2 mm), especially in fine fraction (<0.5 mm). The theoretical optimal size and air flow velocities in Z-shape pneumatic separation is predicted by the sliding mesh method and multiple reference frame technique [39]. The predicted separation efficiency is nearly 100% at size of 3–4 cm and air flow velocities of 6.96–7.8 m/s. Experimental data shows that 99.23% current collectors and 98.64% separators are recycled.

Pneumatic separation with a variable-diameter structure is a novel method to improve separation capacity [40]. The variable-diameter structure accelerates high density particles at the

expanding diameter section and enables particles to rapidly pass through at the reducing diameter section to enhance the capacity of pneumatic separation. Most of the separators and metallic shells are easily removed by pneumatic separation after preliminary crushing by a two-shaft shredder and sieving at 6mm. Then, products are further crushed by a hammer mill and sieved at 2 mm. In the first pneumatic separation, polymer separators are blown out as light products, while the separation efficiency is not provided. In the second pneumatic separation, copper and aluminum are effectively separated with a recovery rate of 92.08% and 96.68%, respectively. It is a good attempt to integrate different separation processes since polymers and Cu/Al are separated using the same system. Unfortunately, the energy consumption for pneumatic separation is not mentioned and impurities besides metals are not evaluated.

In addition, the spouted bed elutriation combined with size separation is used [41]. 52.4% of total polymers are separated from cathode materials or Cu/Al. After comminution in the hammer mill and sieving, components are successively dragged at air velocities of 10.2–10.5 m/s, 10.6–13 m/s, and 13–20.7 m/s in spouted bed elutriation. The elutriation is followed by the second stage size separation to separate polymers, Cu/Al, and the metallic case. The density of the polymer fraction and Cu/Al fraction are 1.66 g/cm^3 and 3.15 g/cm^3 respectively. To improve separation effects, the two-stage size separation and three-stage elutriation are introduced. Simplification and consolidation of these processes should be considered in the future. Unfortunately, the impurities in recycled cathode materials are not mentioned to validate the importance of multi-stage processes.

Currently, Z-shape pneumatic separation is a desirable method to remove polymer separators from metallic components because of its high separation efficiency. Although the modification of z-shape pneumatic separation and spouted bed elutriation are tried, the removal performance of polymers is not well investigated. The influence of polymer separator residue on recycled products used in re-manufactured batteries needs further research.

2.3. Separation of cathode materials from Al/Cu

If cathodes and anodes are crushed together, separation of cathode materials from Al/Cu current collectors is required. The eddy current separation separates non-ferrous metals (copper and aluminum) and cathode materials in LFP-based LIBs [42]. The Al and Cu have good electrical conductivity, generate high intensity eddy current in an alternating magnetic field, and are removed further from the feeding belt. In contrast, LFP has low electrical conductivity, which falls closer to the feeding belt. A force kinematics model based on an iterative method is proposed to predict the motion trajectory of small particles. The Cu and Al are separated at a magnetic roller speed of 800 rpm with maximum particle size ratio of 1.72. This approach can be utilized to harvest ferrous cathode materials (LFP). In other words, it is not suitable for various cathode chemistries. In another study, the magnetic separator followed by eddy current separation separates magnetic and non-magnetic fraction in LCO-based LIBs [43]. The 2.32% Al and 30.35% Co are concentrated in magnetic fraction, and 2.16% Cu is concentrated in non-magnetic fraction. The carbon and plastics are concentrated in non-magnetic fraction. After eddy current separation, the concentration of Al increased to 21.69% in electro-magnetic fraction with decreased Co concentration (5.57%), and Cu increased to 15.72%. The LCO is concentrated in non-electromagnetic fraction. It includes 30% Co,

2% Cu, and 2% Al. The eddy current separation enhances the separation between Cu and Al in electromagnetic fraction, and LCO in non-electromagnetic fraction. The eddy current separation can recycle different components besides cathode materials, but it is not desirable by virtue of high concentration of impurities in recycled products.

The 850 μm cutting point is determined to minimize the involvement of Cu and Al in recycled materials [44]. After shredding by cutting mill and screening to move Fe by magnet roll, products are characterized into four fractions: >2360 μm, 2360–850 μm, 850–38 μm, and <38 μm (Figure 5). For the size fraction <850 μm, the recovery rate of LCO is 43.7% with minimized impurities of 8.8% Al and 10.3% Cu. About 50% of un-reclaimed LCO are in the size fraction >850 um. Unfortunately, the concentration of graphite in recycled products is unknown, and LCO-PVDF aggregates are concentrated together. The average particle size (d_{50}) of spent LIBs is 1552 um. Although the size fraction below 38 μm has less contamination of Al and Cu (1.6% Al and 7.7% Cu), the recovery rate of LCO (11.4%) is far from enough. Interestingly, new LIBs have better mechanical properties of current collectors and adhesiveness of PVDF to prevent breakage of current collectors. Less contaminants (~3% Al and ~2.5% Cu) are found using new LIBs as inputs in size fraction <850 um. In addition, high purity of recycled CAMs in fine particles is noticed in another study. After crushing, magnetic separation, and sieving, 0.4% Cu and 0.54% Al are mixed with cathode materials in the size fraction <0.125 mm [45]. The 11.9% Cu and 16.7% Al are concentrated in overflow fraction (>2 mm), and the underflow fraction (<2 mm) is classified into five fractions: <0.125 mm, 0.125–0.25 mm, 0.25–0.5 mm, 0.5–1 mm, and 1–2 mm. The concentrations of ~5% Cu and ~5% Al are significantly reduced in the size fraction <0.5 m.

Impurities of cathode materials are considered as negative factors in direct recycling due to the unstable electrochemical performance of LIBs made from recycled CAMs. The separation between cathode materials and current collectors (Al and Cu) after comminution is not complete. The elements distribution by particle size are shown in Figure 6 [46]. After magnetic separation to move iron scraps, ~80% of Al and Cu are in the particle fraction 2–6.7 mm, and 33–45% of the total cathode materials is removed with current collectors after sieving.

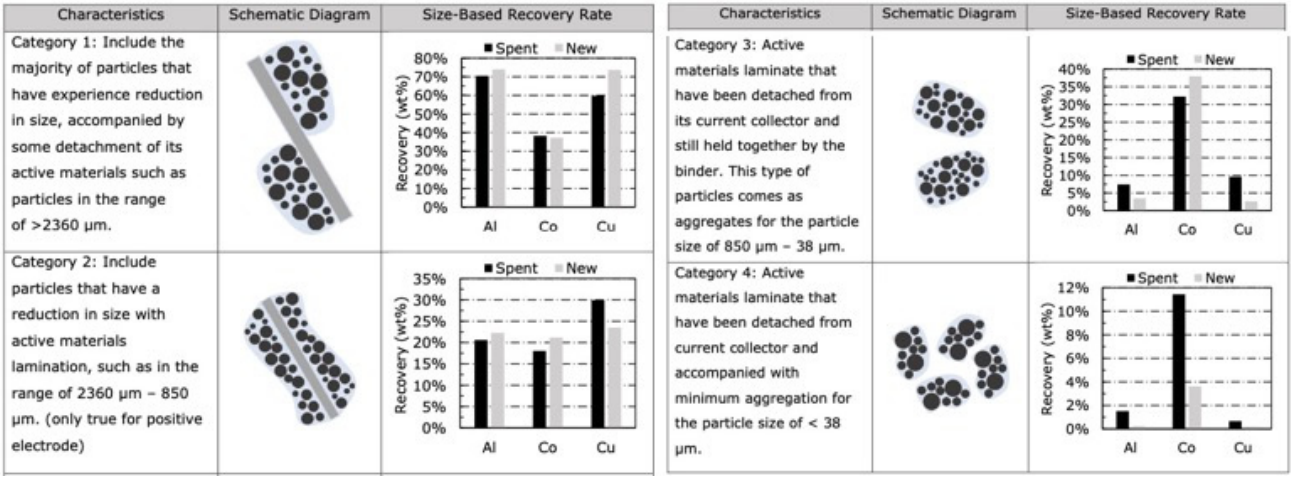

Figure 5. Characterization of classified lithium-ion battery powder [44].

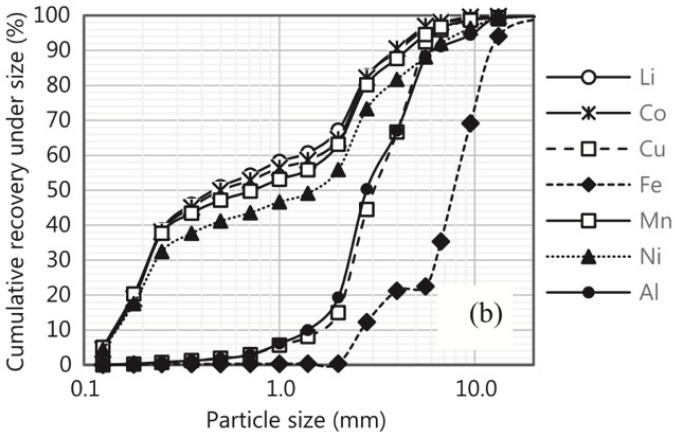

Figure 6. Distribution of the elements by particle size [46].

3. Delamination of cathode materials from cathode

Crushing of batteries cells, cathode/anode sheets, or cathode sheets alone could induce many contaminants such as Cu, Al, and graphite. Delaminating the cathode layer from the Al current collector can address this issue. The ideal recycled products are cathode material powders, which are easier to process further. The difficulties come from the strong binding forces provided by PVDF, which is chemical corrosion resistant and thermal resistant. The binding forces come from two aspects: (1) mechanical interlocking forces between cathode layer and Al foil (current collector); and (2) forces among CAMs [47,48]. The technologies include dissolution of PVDF, decomposition of PVDF, and dissolution of Al foil. It is important to mention that residues of PVDF and carbon black may exist in recovered products. In direct recycling processes involving comminution, the Al foils and cathode materials are completely mixed because they are both powders. In contrast, the distinct nature of recycled products (Al is separated as pieces, and recycled cathode materials could be powders or pieces) after delamination enables simple separation to harvest Al or cathode materials. Al foils are easily taken out using tweezers. Therefore, the separation approaches after comminution (crushed Al and crushed CAMs) are different from those after delamination. Currently, delamination of cathode materials from cathode is in laboratory stage, and scaling-up processes after delamination need further research.

The solubility behavior of PVDF in 46 solvents and their Hansen solubility parameters are investigated [49]. Four effective solvents are widely used in LIBs recycling to remove PVDF: N-methyl-2-pyrrolidone (NMP), N-N-dimethylformamide (DMF), N-N dimethylacetamide (DMAC), and N-N-dimethyl sulfoxide (DMSO) [50–53]. These four solvents (NMP, DMF, DMAC, and DMSO) and ethanol are compared in terms of separating cathode materials from cathode to recycle $LiCoO_2$ [54]. In addition, the ultrasound technology is applied to enhance the peel-off efficiency at least 6 times. The mechanism can be explained by facilitated convective motion of solvent and ultrasonic cavitation caused by compression and rarefaction cycles. The optimal conditions are 240 W of ultrasonic power, temperature of 70°C, and reaction time of 90 min. The effectiveness from

high to low is NMP > DMAC > DMF > DMSO > ethanol. However, the air pollution resulting from volatilization of organic solvents is cause for concern.

Other solvents are studied in order to minimize environmental impacts. Cyrene, a biodegradable solvent, is able to dissolve PVDF and achieves separation at 80°C after 1 hour with solid-to-liquid ratio of 500 g/L [55]. The phase separation between PVDF and Cyrene after cooling enables them to be recycled. However, the organic film (3.3 wt%) that covers the surface of recycled CAMs changes the morphology. In another study, a thermal stable and low vapor pressure [BMIm][BF_4] ionic liquid is proposed to replace NMP and recycle cathode materials [56]. 99% of LCO CAMs can be recycled at 180°C for 25 min with 300 rpm rotation, but the price of reagents leads to scale-up problems.

Some approaches can break the binding force between the cathode layer and Al foil. Because the binding forces among CAMs particles provided by PVDF are not broken, the cathode layers are recycled as small pieces. Choline chloride and glycerol as deep eutectic solvents can peel off 99.87% NMC111 cathode materials at 190°C after 15 min [57]. The deactivation mechanism is based on hydrogen bond formation, e.g., between hydrogen atoms in -CH_2- group of PVDF and electron-withdrawing group of choline chloride, and between -CF_2- group of PVDF and electron-donating group of glycerol, and degradation of PVDF. In another study, the time of delamination is significantly decreased. Bai et al. found that ethylene glycol can peel off NMC523 in 6 seconds (solid-to-liquid ratio is 1:10 at 160°C) [58]. To the best of our knowledge, this is the fastest way to delaminate cathode layers. The separation time is independent of the size of cathode pieces owing to rapid diffusion of solvent and porous nature of cathode. The authors propose that delamination of cathode layer relies on strong hydrogen bond formation between ethylene glycol and the oxidation layer of Al foil and replacement of binding forces between PVDF and Al foil. This mechanism cannot explain why water with higher strength of hydrogen bonding (42.3 $MPa^{1/2}$), which is easier to form hydrogen bonds and replace binding forces between PVDF and Al foil, is not as effective as ethylene glycol (26 $MPa^{1/2}$). The reagents for delamination can be made from waste oil. Thus, the environmental impacts from chemicals are reduced. The waste oil, methanol, and NaOH are used to produce fatty acid methyl esters (FAME) [59] as a transition solvent to dissolve PVDF. The cross-linking of hydrogen bonds between FAME and PVDF leads to exfoliation of the cathode layer. 99.1% of the cathode layer can be stripped from Al foil at 190°C for 20 min. A study demonstrates that no chemicals are needed for the separation of LCO-based cathodes. The low temperature can deactivate PVDF and achieve separation [60]. The 87.29% LCO is recycled after the pre-freezing stage at 77 K for 5 min and low temperature grinding stage for 30 seconds. Small cracks are noticed between the cathode layer and Al foil and in the cathode layer. Liquid nitrogen is needed to provide low temperatures, resulting in hidden risks and costs during maintenance.

An alternative approach to achieve delamination of cathode layer is to use molten salts to deactivate or decompose PVDF. A molten aluminum chloride-sodium chloride ($AlCl_3$-NaCl) system is employed to deactivate PVDF in $LiCoO_2$ cathode layer [61]. 99.8% peel-off efficiency is achieved at the following optimal conditions: temperature of 160°C, holding time of 20 min, $AlCl_3$-NaCl molar ratio of 1:1, and salts-to-cathode mass ratio of 10. The $AlCl_3$-NaCl system serves as heat storage and melts at 154°C, and the system is able to transfer heat and melt PVDF (melting point of 172°C) at 160°C. The reagent cost is $0.67/kg cathode. The bonds between cathode layer and Al foil are broken. It should be noted that this approach induces other cations such as aluminum and sodium.

To avoid this problem, Ji et al. apply lithium salts to recycle heterogenuous cathode materials (NMC111 and LMO) [62]. Binary eutectic systems formed by three common lithium compounds (LiCl, $LiNO_3$, and LiOH) are compared. Unlike cathode pieces from $AlCl_3$-NaCl treatment, the cathode layer is converted to powders after LiOH-$LiNO_3$ treatment, indicating that bonds among CAMs are broken at 260°C and 30 minutes. Therefore, the subsequent mechanical separation is not required. The melting LiOH-$LiNO_3$ provides sufficient contact area and promotes decomposition of PVDF by capturing released HF. H_2O and alkylamines are decomposition products of PVDF.

PVDF can also be thermally decomposed in the temperature range of 350–600°C. Cathode sheets or cathode scraps are directly calcinated at 500–600°C to decompose PVDF and harvest CAMs [63–66]. The decomposition products of PVDF are toxic hydrogen fluoride, highly fluorinated hydrocarbons such as C_2HF, $C_6H_4F_3$, and $C_8H_6F_5$, hydrocarbons such as C_2H_6 and C_3H_6, and other gases, e.g., H_2 and CO_2 [67,68]. Calcium oxide can be used to capture HF and promote the decomposition of PVDF [69], while minimizing environmental impacts from HF release. Compared with thermal decomposition of PVDF at 500°C, using CaO decreases the reaction temperature to 300°C (chemicals-to-cathode mass ratio of 8 and holding time of 30 min). The hydrocarbons (C_nH_m) and H_2 are identified as other decomposition products. The economic analysis shows that the cost of $0.5/kg NMC111 could be saved in terms of decreased reaction temperature. The profit is $0.3/kg of NMC111. The recycled products have minimal morphological or structure changes.

It is also possible to use NaOH to separate Al and cathode layer since Al can dissolve in NaOH solution while cathode materials do not. In one study, after shredding, the cathode mixture is dissolved in 2 M NaOH solution for hours to remove Al [35,63]. In another study, 98% of Al is dissolved in 10 wt% NaOH solution at solid-to liquid ratio of 1:10 after 5 hours, and little Co and Cu are detected in alkali solution [70]. He et al. use Na_2SiO_3 and Na_2CO_3 solution to remove around 63.2 nm depth of Al and achieve separation at pH value of 11.6 [48]. Na_2SiO_3 is added to minimize the dissolution of Al.

4. Recovery of cathode active materials

The recycled cathode materials may include CAMs, PVDF, and graphite/acetylene black. The next step is to collect CAMs and remove other components. Two approaches are discussed. Impurities can be directly calcinated at a high temperature. The released gases contain, but are not limited to, carbon dioxide and hydrogen fluoride. In contrast, flotation based on differences in surface hydrophobicity produce significantly minimal gas emission and recycled anode materials during CAMs, PVDF, and graphite/acetylene black separation [71,72]. The collectors and frothing agents are added to enhance the wetting differences of impurities and CAMs.

4.1. Thermal treatment

Thermal treatment is widely used to remove residues of PVDF and graphite/acetylene black. PVDF is decomposed in the temperature range of 350–600°C [50,62,63], and carbon is decomposed in the temperature range of 600–800°C [65,73]. The TGA curves of electrode components are shown in Figure 7. To avoid the influence of PVDF or carbon in the making of new batteries cells, the CAM

is calcinated at ~800°C before or after regeneration, which is also known as the annealing process. Besides toxic gases released from PVDF, carbon dioxide emission from thermal treatment is significant. The vacuum pyrolysis is used to decompose the binder in mixed cathodes from different battery types. Xiao et al. mix three kinds of LIBs: 18650 type (laptop computers, LMO), lump type (mobile phones, LCO), and brick type (EVs, NMC), where polyvinyl alcohol is used as binder [74]. The mixed powder is crushed and screened (<0.12 mm). The binder is removed under vacuum (<1000 Pa) pyrolysis (>300°C).

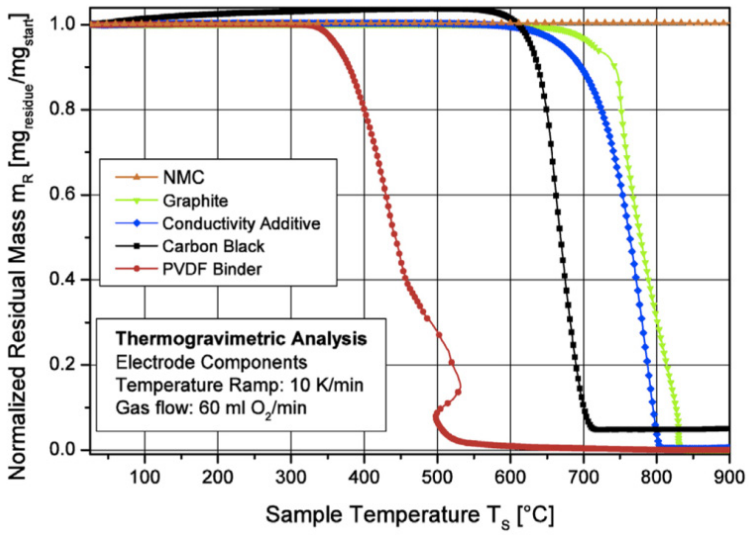

Figure 7. TGA curve of electrode components [75].

Nie at al. propose the process to obtain recycled CAMs: Al is sieved after decomposition of PVDF at 400°C with 50 mesh screen, and carbon is removed after decomposition at 800°C with 400 mesh screen [73]. In order to minimize the emission, froth flotation combined with pyrolysis is studied to separate LCO and PVDF/carbon. The electrode scraps are treated by pyrolysis to remove PVDF binder at 550°C for 15 minutes [76]. Flotation is applied after the pyrolytic process using 300 g/t n-dodecane and 150 g/t methyl isobutyl carbinol. Although organic matters can sufficiently decompose at 500°C, the wetting difference between anode and cathode materials is more obvious at 550°C: the contact angle of anode materials is 69° and that of cathode materials is 33° (Figure 8). The anode concentrates are collected as froth products and 94.97% cathode concentrates are collected as tailing products. Because 15.63% of the cathode is left as a remainder in froth products, multi-stage flotation should be conducted to improve CAMs recovery.

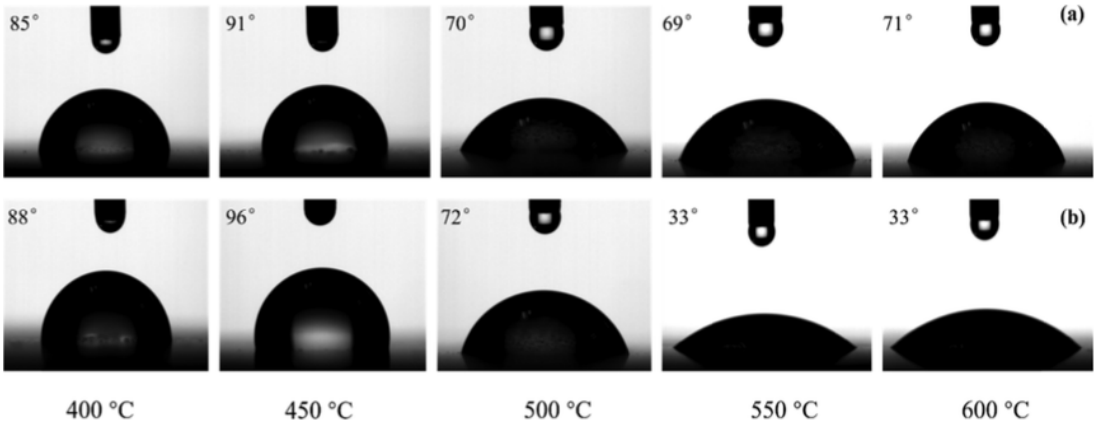

Figure 8. Contact angles of the pyrolytic electrode materials at different pyrolysis temperatures: (a) anode material and (b) cathode material [76].

4.2. Flotation

Flotation is used to minimize gas emissions when achieving separation between CAMs and carbon with additive collectors and frothing agents [71,72]. No HF is released from PVDF during flotation. Two-step flotation is proposed to separate LCO CAMs and graphite [30]. After crushing and screening, the cathode and graphite powder are mixed in the particle size of <0.074 mm. The anode and cathode concentrates are collected from the froth product and tailing product, respectively. The methyl isobutyl carbinol as collectors and n-dodecane as frothing agents are added to enhance the hydrophobicity of graphite in the first step and hydrophilicity of LCO in the second step, respectively. Due to significant wetting differences, 73.56% graphite is collected as floats and 97.13% LCO is collected as sediments.

Flotation can separate CAMs from carbon as well as CAMs from PVDF and carbon. Another study applies two step flotation to effectively remove residues of PVDF and carbon black (acetylene black) [77]. First, the cathode materials are agitated with water for 5 to 10 s in the delamination process. After wet sieving to remove Al, the de-agglomeration process is carried out in a commercial blender at a tip speed of 90–100 m/s. The particle size is decreased to 10 μm. The froth flotation is based on the differences in surface wetting and density between CAMs and PVDF/carbon black. The CAMs are naturally hydrophilic, and PVDF/carbon black are hydrophobic [78,79]. Kerosene is used to enhance hydrophobicity of the impurities. In addition, the density differences between CAMs and PVDF/carbon black promotes the separation: density of CAMs is ~5 g/cm^3 and density of PVDF and carbon black are 1.78 g/cm^3 and 1.7 g/cm^3, respectively. After a 16-min deagglomeration process, the tailing contains less than 2% of carbon black/PVDF and 89.7% of CAMs are recycled. Froth flotation should be applied multiple times to increase separation effects.

The Fenton reaction-assisted flotation process removes organic compounds outer layer, which reduce wettability difference between LCO and graphite [80]. The outer layer (2% phosphates, 5% of metal oxides and 6% of metal fluorides) is oxidized by the Fenton process, e.g., PVDF is oxidized into small molecules, and organic matters are decomposed to carbon dioxide and water. The

parameters — H_2O_2/Fe^{2+}, pulp density, impeller speed, pH, and aeration — are optimized at 1:120, 40 g/L, 1800 rpm, 9, and 0.8 L/min. After flotation (300 g/t n-dodecane as collector and 150 g/t methyl isobutyl carbinol as frothing agents), the recovery rate of LCO and graphite are 39.6% and 16.77% respectively. In concentrates, the enrichment ratios of Co, Mn, Cu, and Al are 1.41, 1.27, 1.35, and 1.25 with 2.33 wt% of carbon (EDS).

5. Regeneration

Direct recycling technologies generally require regeneration to improve the electrochemical performance of spent cathodes through restoration of their composition and crystal structure. The main issue with cathodes from spent LIBs is capacity loss. Many studies find active lithium loss as one of the main reasons that leads to capacity loss in LIBs [81–84].The reasons could be surface degradation during cell operation, surface impurities' parasitic reactions, and electrolyte interface layer formation [85,86].

The lithium salts and lithium hydroxide as lithium resources show the potential to recover degraded CAMs to achieve their original stoichiometric ratio and crystal structure, and to make their rate capacity and cycling stability comparable to pristine cathodes. Regeneration in direct recycling technologies mainly includes two approaches: solid-state re-lithiation or hydrothermal re-lithiation. One of the main differences is that either solid state lithium reagent or lithium hydroxide solution is used as a lithium resource. Because of different cathode chemistries, the operation conditions of regeneration vary in terms of cathode. In addition, other processes including ionic liquid, electrochemical process, and synthesis of new cathode are summarized. The raw materials are spent CAMs with or without PVDF and carbon. The co-precipitation, sol-gel method, and carbon-thermal reduction method, where fabricated cathode materials powder through pretreatment process are dissolved in acid solution, are considered as regeneration for hydrometallurgical recycling rather than direct recycling [87]. Therefore, these approaches are not included in this review.

5.1. Solid-state re-lithiation

Solid-state re-lithiation applies solid state lithium reagents as lithium resources. Lithium ions are incorporated into available sites at high temperature and are used to compensate lithium loss after charge-discharge cycling. The lithium resources could be lithium carbonate, lithium nitrate, and lithium hydroxide. The operational conditions of solid-state re-lithiation, and initial discharge capacity and capacity retention of regenerated CAMs are summarized in Table 1.

Nie et al. propose using Li_2CO_3 to synthesis LCO and generate LCO [73]. The regenerated LCO meets the commercial requirements for reuse. The spent LCO CAMs is directly calcinated with Li_2CO_3 at 900°C for 12 hours. The initial discharge capacity of recycled LCO is 152.4 mAh g^{-1} with attenuation rate of 0.0313 mAh g^{-1} in 80 cycles. The similar regeneration is investigated by Shi et al. using Li_2CO_3 at 850°C for 12 hours [88]. The discharge capacity of recycled LCO is 152.1 mAh g^{-1} (retention rate of 89%) after 100 cycles. These two researchers both apply molar ratio between Li and Co is 1.05:1 (5% Li excess), and input Li_2CO_3 should be accurate to avoid over-lithiated or under-lithiated LCO [94]. The metallic composition analysis is required before experiments to

determine the Li/Co ratio from cell to cell. In addition, $Li_{\chi}CoO_2$ decomposes to Co_3O_4 and releases O_2, then Li_2CO_3 reacts with Co_3O_4 and forms $LiCoO_2$. The melting of salt facilitates the re-lithiation and improves the cycling stability. The melting point of Li_2CO_3 is 723°C. If reaction time is below 723°C, the recycled products show poor cycling stability. For example, the discharge capacity of CAMs recycled at 700°C is 111.1 mAh g^{-1} with retention rate of 74.2% after 100 cycles. The reactions are listed as following [95,96]:

$$Li_{\chi}CoO_2 \rightarrow \frac{1-\chi}{3}Co_3O_4 + \chi\ LiCoO_2 + \frac{1-\chi}{3}O_2$$

$$2Co_3O_4 + 3\ Li_2CO_3 + \frac{1}{2}O_2 \rightarrow 6\ LiCoO_2 + CO_2$$

Table 1. The operational conditions of solid-state re-lithiation, and initial discharge capacity and capacity retention of regenerated cathode active materials.

Cathode	Conditions	Annealing process	Discharge capacity 1st (mAh g^{-1})	Capacity retention (Discharge capacity mAh g^{-1})	Reference
LCO	Mixed with Li_2CO_3 by ball mill at 900°C for 12 h	-	152.4	149.9 (3−4.3 V at after 80 cycles)	[73]
LCO	Li_2CO_3 at 850°C for 12 h	-	152.1 (C/10)	135.4 (3−4.3 V at 1 C after 100 cycles)	[88]
NMC111 NMC523	Sintered with Li_2CO_3 at 850°C for 4 h in oxygen	-	153.3 ~160 (C/10)	125.4 127.4 (3–4.5 V at 1C after 100 cycles)	[89]
NMC	Mixed with Li_2CO_3 by ball mill (Mechanochemical activation)	Sintered with Li_2CO_3 at 800°C for 10 hours	165	133.3 (2.5−4.3 V at 0.2 C after 100 cycles)	[90]
LFP	Li_2CO_3 at 650°C for 1h	-	147.3	140.4 (2.5−4.2 V at 0.2 C after 100 cycles)	[91]
NMC523	$LiNO_3$: LiOH = 3:2 at 300°C, 2 hours	Sintered with Li_2CO_3 at 850°C for 4 h	149.3 (C/10)	134.6 (3−4.3 V at 1 C after 100 cycles)	[92]
LMO	LMO: LiOH = 1:1 at 350°C for 24 hours	750°C, 6 hours	~35	~35 (C/6 after 10 cycles)	[93]

In addition, Li_2CO_3 can be used to regenerate NMC CAMs at 850°C [89]. Mechanical activation is combined with the solid-state process in order to accelerate the diffusion of lithium ions [90]. Li_2CO_3 is used as lithium resource. After mechanical activation, the mixture of NMC and Li_2CO_3 is sintered at temperatures of 800°C for 10 hours. With the help of mechanical activation and sintering, the discharge capacity of NMC improves and the layered structure is restored resulting from the decreased content of nickel and cationic disordering. This result emphasizes the importance of controlling the ratio between additive lithium and CAMs.

Li_2CO_3 also works for LFP-based cathode re-lithiation. Li et al. apply Li_2CO_3 to generate $LiFePO_4$ at 650°C for 1 hours [91]. The reaction time of regeneration LFP is much shorter compared with NMC. The particle size (D50) decreases with elevated temperature, but high temperatures (700–800°C) lead to decreased tap density resulting from decomposition of resynthesized LFP. A direct recycling flow diagram is proposed. Unfortunately, some operational conditions of other processes are not mentioned, such as centrifugal speed and concentration of NaOH solution to separate cathode materials.

The salt mixture of $LiNO_3$ and LiOH at the molar ratio of 3:2 that has the lowest melting point of 175°C, are used to synthesize NMC111 cathode [97]. This eutectic system is promising to achieve re-lithiation at low temperature. LiOH-$LiNO_3$ ambient-pressure re-lithiation with an annealing step is able to restore 50% capacity loss of spent NMC523 (149.3 mAh g^{-1}) to the level of pristine materials (146.6 mAh g^{-1}) [92]. In addition, the cycling stability and rate capacity are improved because of compensation in lithium loss. It is important to mention that phase change on the surface or subsurface of NMC523 is reversed if lithium ions are incorporated to their original sites.

The lithiation of degraded NMC523 are listed as follows:

$$Li_{1-x}Ni_{0.5}Co_{0.2}Mn_{0.3}O_2 + x\ LiOH \rightarrow LiNi_{0.5}Co_{0.2}Mn_{0.3}O_2 + \frac{x}{2}H_2O + \frac{x}{4}O_2$$

$$Li_{1-x}Ni_{0.5}Co_{0.2}Mn_{0.3}O_2 + x\ LiNO_3 \rightarrow LiNi_{0.5}Co_{0.2}Mn_{0.3}O_2 + x\ NO_2 + \frac{x}{2}\ O_2$$

As we mention before, one study approves that LiOH-$LiNO_3$ molten salt can peel off NMC111 and LMO cathode materials from cathode without damaging Al foil at 260°C for 30 minutes [62]. Therefore, the separation of cathode materials and regeneration of CAMs can be finished in one step. Even though the recycled product is the mixture of regenerated CAMs, undecomposed PVDF residues, and carbon, they can be separated with processes mentioned in the previous section. It provides a promising sustainable approach for spent cathode recycling.

However, LiOH solid-state for LMO re-lithiation is not satisfied. The aged LMO is mixed with LiOH and heated at 350°C for 2 hours to obtain intermediate products [93]. Because it is hard to control the stoichiometric ratio between solid LMO and solid LiOH, the intermediate products can be over-lithiated or under-lithiated. Therefore, an energy-intensive subsequent process (750°C for 6 hours) is required to decompose over-lithiated LMO. The electrochemical performance of the final product (discharge capacity of 35 mAh g^{-1}) is far from pristine LMO (90 mAh g^{-1}). The decomposition of over-lithiated LMO is listed as following:

$$Li_{1+x}Mn_{2-x}O_4 \rightarrow z\ Li_2MnO_3 + (1-z)\ Li_{1+y}Mn_{2-y}O_4 + \frac{z}{2}O_2\ \ y=(x-z)/(1-z)$$

5.2. Hydrothermal re-lithiation

Hydrothermal re-lithiation uses lithium hydroxide solution as lithium resource, and it is commonly followed by an annealing process at 800°C. Some technologies are involved to accelerate lithium ions transfer such as ultrasonication and aqueous pulsed discharge plasma. The operational conditions of hydrothermal re-lithiation, and initial discharge capacity and capacity retention of regenerated CAMs are summarized in Table 2.

Table 2. The operational conditions of hydrothermal re-lithiation, and initial discharge capacity and capacity retention of regenerated cathode active materials.

Cathode	Conditions	Annealing process	Discharge capacity 1st (mAh g^{-1})	Capacity retention (Discharge capacity mAh g^{-1})	Reference
LCO	1 M LiOH and 1.5 M Li_2SO_4 at 220°C for 4 hours	800°C, 4 hours	148.2 (C/10)	135.1 (3−4.3 V at 1 C after 100 cycles)	[88]
LCO	2 M LiOH at 220°C, ultrasonication 999 W, 10 hours	-	131.5	129 (3−4.5 V after 20 cycles)	[98]
LCO	0.1 M LiOH with aqueous pulsed discharge plasma	-	132.9 (C/5)	126.7 (2.8−4.2 V at C/5 after 50 cycles)	[99].
NMC111 NMC523	LiOH at 220°C for 4 hours	Li_2CO_3 at 850°C, 4 hours	158.4 175 (C/10)	122.6 128.3 (3−4.2 V at 1C after 100 cycles)	[89]
LMO	0.1 M LiOH at 180°C for 2 hours	-	111 (C/10)	98 (3.0−4.3 V at 0.5 C for 100 cycles)	[100]
LMO	LMO:LiOH = 1:1 at 165°C for 24 hours	-	~98	~95 (after 10 cycles)	[93]

Shi et al. propose a two-step hydrothermal regeneration process to improve the electrochemical performance of recycled LCO [88]. The solution includes 1 M LiOH and 1.5 M Li_2SO_4 to decrease the pH = 12.3 (or 4 M LiOH) and provides sufficient lithium ions at the same time. The solution is heated at 220°C for 4 hours. After that, the cathode materials are annealed at 800°C for 4 hours. The discharge capacity is 135.1 mAh g^{-1} with retention rate of 91.2% after 100 cycles. In terms of the specific capacity or cycling stability, there are not significant differences between the samples from solid-state regeneration by Li_2CO_3 and those from hydrothermal regeneration followed by an

annealing process. For example, the initial discharge capacity (cycle at C/10) of recycled LCO from solid-state and two-step hydrothermal regeneration are 152.1 mAh g^{-1} and 153.1 mAh g^{-1}, respectively. However, the hydrothermal processes are easier to operate and control the concentration between CAMs and additive lithium ions.

The ultrasonic regeneration is combined with hydrothermal re-lithiation to recycle LCO. The discharge capacity of renovated LCO is 129 mAh g^{-1} with retention rate of 98.1% after 20 cycles [98]. The conditions are 2 M LiOH solution, heating temperature of 120°C, ultrasonic system of 999W, reaction time of 10 hours, and solid-to-liquid ratio of 14.3 g/L. Unfortunately, the specific capacity (132.6 mAh g^{-1}) is not comparable to the pristine LCO. The energy consumption from ultrasonic system is not negligible, and the effectiveness of said system to improve the lithium transfer efficiency is not confirmed.

Zhu et al. make an interesting attempt using 0.1 M lithium hydroxide solution combined with aqueous pulsed discharge plasma to renovate spent LCO [99]. The renovated LCO has initial discharge capacity of 132.9 mAh g^{-1} with retention rate of 97.2% after 50 cycles. Free radicals and cavitation bubbles provided by a pulsed high voltage system facilitate PVDF and organic electrolyte decomposition and heat/mass transfer in the renovation process, respectively. Electrohydraulic cavitation, however, causes a high-energy (~4850°C) chemical reaction which leads to the melting of $LiCoO_2$ and cation rearrangement resulting in order-disorder transition for the hexagonal phase.

The two-step LiOH solution regeneration (a hydrothermal treatment followed by an annealing process) is also used to regenerate NMC cathode (NMC111 and NMC523). The recycled cathode is hydrothermally treated in lithium hydroxide solution at 220°C and 10 MPa for 4 h, followed by annealing at 850°C for 4 hours in Li_2CO_3 [89]. The specific capacity and capacity retention of regenerated NMC samples through solid-state and hydrothermal regeneration are similar, such as the capacity retention of NMC523 (127.4 mAh g^{-1} in solid-state treatment and 128.3 mAh g^{-1} in hydrothermal treatment after 100 cycles). However, the hydrothermal reatment provides better cycling performance. The high-pressure operation leads to additional cost and safety concerns.

In terms of LMO cathode, one-step hydrothermal regeneration is enough. Gao et al. achieve re-lithiation of LMO by heating LMO cathodes in 0.1 M LiOH solution at 180°C for 12 hours (the solid-to-liquid ratio is 3.125 g/L) [100]. The capacity and cycling stability are comparable or superior to pristine LMO. For example, the capacity retention of pristine LMO is 86.6% after 100 cycles, and it increases to 88% after regenerated in 0.1 M LiOH. If LiOH solution is used to re-lithiate LMO, the concentration of LiOH is more important than the reaction temperature or reaction time [93]. The initial discharge capacity is ~98 mAh g^{-1} using LMO to LiOH molar ratio of 1:1. A high concentration of LiOH (LMO:LiOH = 10:1) results in Li_2MnO_3 impurity, and high or low concentration (LMO:LiOH = 1:10) may lead to transfer or decomposition of LMO.

5.3. Other regeneration processes

The ionic liquid provides thermal stability and synthesis flexibility as flux medium or reaction possibility to solid-state CAMs generation. The spent NMC is mixed with lithium resource (LiBr) and imidazolium ionic liquid at 150°C for 6 h [101]. The initial charge capacity of recycled NMC is 173.6 mAh g^{-1} (3−4.3 V at C/10), which is as good as pristine cathode (175.3 mAh g^{-1}). LiOAc,

LiNTf, LiBr, and LiCl are tested as lithium resources. Among these four lithium sources, LiBr is superior. This is because Br^- is easier to be oxidized (Br^-/Br_2 1.065 V), and formation of Br_2 is removed from the system, thus facilitating the lithiation reaction. Large scale (25 g) NMC cathode is applied to reduce the amount of ionic liquid, which is the major contributor to the total cost. 98.9% ionic liquid can be recycled in large scale.

An electrochemical process is proposed to minimize the production of waste and input reagents. The electrochemical regeneration can insert lithium ions to waste $LixCoO_2$ electrode, where waste $LixCoO_2$ as cathode, platinum as anode, and Li_2SO_4 solution as electrolyte [102]. The operational conditions are cathodic current density of −0.42 mA cm^{-2}, reaction time of 100 minutes, and Li_2SO_4 concentration of 1 M. The recycled products should be annealed at 700°C for 2 hours. These two processes call for high energy consumption. The charge capacity of regenerated LCO cathode (136 mAh g^{-1}) is close to commercial $LiCoO_2$ (140 mAh g^{-1}). This study also finds that the re-lithiation rate at high concentration, e.g., no less than 0.5M, of electrolyte is controlled by charged transfer, and it controlled by mass diffusion at low concentration of electrolyte (<0.3 M of electrolyte).

Besides relithiation, refreshing approach is studied to obtain high charge-discharge efficiency and good cycling performance of CAMs (the mixture of NMC523 and LMO) [103]. New lithium manganate coating layer is formed on recycled cathode materials. The specific discharge capacity is 152.6 mAh g^{-1} (2.5−4.3 V at 1C after 100 cycles), and the capacity retention ratio is 79.1%. Without dissolution of recycled cathode material, manganese hydroxide coating is formed on the surface of cathode material by additive manganiferous salt and alkali solution. Then, lithium hydroxide is used to produce lithium manganate coating layer. This refreshing approach provides another way of regeneration by producing a new cathode active material on recycled cathode materials to compensate for the degraded performance of used LIBs.

6. Challenges and future research

The crushing of electrodes (cathode and anode) or LIBs cell is well studied. Polymers can be removed from cathode materials and Al/Cu mixtures by Z-shape pneumatic separation. It is known that CAMs and carbon (graphite and acetylene black) are concentrated in fine particle fraction and Al/Cu are enriched in large particle fraction. We need to balance the improvement of CAMs recovery rate and involvement of more Cu or Al impurities. In order to minimize the induction of aluminum and copper, the exfoliation of cathode materials from cathode must be successfully achieved. Manual dismantlement to remove separators and anode sheets is required to obtain cathode sheets. It is desirable to have an automated separation process to harvest cathode sheets. Except for thermal treatment, complete separation between CAMs and PVDF/carbon is not found. The exiting of residues of PVDF or carbon may affect the electro-chemical performance of manufactured new cells from spent CAMs. Based on the current situation, manual dismantlement limits the possibility of scaling up. Having various configurations, pouch cells may require different automatic disassembling processes, which are difficult to operate. Therefore, crushing battery cells at the beginning, which is followed by polymer separation, current collector separation, and carbon and PVDF separation, is more promising to scale up.

In terms of regeneration, many efforts have been made towards re-lithiation of degraded CAMs. Homogeneous cathodes, e.g., LCO, NMC, LMO, and LFP are successfully regenerated by solid-state re-lithiation or hydrothermal re-lithiation. Regeneration of heterogeneous cathodes such as the mixture of NMC and LMO cathode has not be studied, which should be more complicated than homogeneous cathode regeneration. Lithium salts are commonly used lithium resources to compensate for lithium loss. The influences of anions in lithium chemicals on regeneration are unknown. Since lab-made battery cells are used to test regenerated CAMs, the ratio among recycled CAMs, PVDF binder, and carbon black will affect the results. Therefore, the electrochemical performance results from different studies cannot be compared.

EverBatt is a powerful Excel-based model developed by Argonne National Laboratory to evaluate cost and environmental impacts for many lifecycle stages of LIBs including recycling [104]. In addition, NREL's Battery Second-Use calculator explores benefits of repurposing LIBs [105]. We recommend that both economic and environmental evaluations should be made for novel recycling technologies and a comparison should be considered for some similar technologies to obtain the same end-products. For example, in the study of Shi et al., there are no significant electrochemical performance differences of regenerated LCO in terms of specific capacity or cycling stability by solid-state regeneration and hydrothermal regeneration [88]. The better one should be selected in terms of eco-environmental analysis. It is known that recycled cathode should have the same cathode chemistry as the original CAMs. Because of the rapid changes in cathode components and configuration of LIBs, we need to consider how to handle different cathodes or batteries cells together in direct recycling.

Acknowledgments

This work was supported by the Critical Materials Institute, an Energy Innovation Hub funded by the U.S. Department of Energy, Office of Energy Efficiency and Renewable Energy, Advanced Manufacturing Office.

Conflict of interest

Authors declare that there is not conflict of interest.

References

1. Wang Y, Liu B, Li Q, et al. (2015) Lithium and lithium ion batteries for applications in microelectronic devices: A review. *J Power Sources* 286: 330–345.
2. Jones B, Elliott RJR, Nguyen-Tien V (2020) The EV revolution: The road ahead for critical raw materials demand. *Appl Energy* 280: 115072.
3. Jacoby M (2019) It's time to get serious about recycling lithium-ion batteries. *Chem Eng News* 28.
4. Turcheniuk K, Bondarev D, Singhal V, et al. (2018) Ten years left to redesign lithium-ion batteries. *Nature* 559: 467–470.

5. Lv W, Wang Z, Cao H, et al. (2018) A Critical Review and Analysis on the Recycling of Spent Lithium-Ion Batteries. *ACS Sustainable Chem Eng* 6: 1504–1521.
6. Richa K, Babbitt CW, Gaustad G, et al. (2014) A future perspective on lithium-ion battery waste flows from electric vehicles. *Resour Conserv Recycl* 83: 63–76.
7. Winslow KM, Laux SJ, Townsend TG (2018) A review on the growing concern and potential management strategies of waste lithium-ion batteries. *Resour Conserv Recycl* 129: 263–277.
8. Lagadec MF, Zahn R, Wood V (2018) Characterization and performance evaluation of lithium-ion battery separators. *Nat Energy* 4: 16–25.
9. Aravindan V, Gnanaraj J, Madhavi S, et al. (2011) Lithium-Ion Conducting Electrolyte Salts for Lithium Batteries. *Chem A Eur J* 17: 14326–14346.
10. Zhang SS (2006) A review on electrolyte additives for lithium-ion batteries. *J Power Sources* 162: 1379–1394.
11. Xie J, Lu YC (2020) A retrospective on lithium-ion batteries. *Nat Commun* 11: 2499.
12. Li M, Lu J, Chen Z, et al. (2018) 30 Years of Lithium-Ion Batteries. *Adv Mater* 30: 1800561.
13. Dunn JB, James C, Gaines L, et al. (2015) Material and Energy Flows in the Production of Cathode and Anode Materials for Lithium Ion Batteries. Argonne National Lab. (ANL), Argonne, IL (United States).
14. Ponrouch A, Palacín MR (2011) On the impact of the slurry mixing procedure in the electrochemical performance of composite electrodes for Li-ion batteries: A case study for mesocarbon microbeads (MCMB) graphite and Co3O4. *J Power Sources* 196: 9682–9688.
15. Ludwig B, Zheng Z, Shou W, et al. (2016) Solvent-Free Manufacturing of Electrodes for Lithium-ion Batteries. *Sci Rep* 6: 23150.
16. Guerfi A, Kaneko M, Petitclerc M, et al. (2007) LiFePO4 water-soluble binder electrode for Li-ion batteries. *J Power Sources* 163: 1047–1052.
17. Kim S, Bang J, Yoo J, et al. (2021) A comprehensive review on the pretreatment process in lithium-ion battery recycling. *J Cleaner Prod* 294: 126329.
18. Gaines L (2019) Profitable Recycling of Low-Cobalt Lithium-Ion Batteries Will Depend on New Process Developments. *One Earth* 1: 413–415.
19. Makuza B, Tian Q, Guo X, et al. (2021) Pyrometallurgical options for recycling spent lithium-ion batteries: A comprehensive review. *J Power Sources* 491: 229622.
20. Zhang X, Li L, Fan E, et al. (2018) Toward sustainable and systematic recycling of spent rechargeable batteries. *Chem Soc Rev* 47: 7239–7302.
21. Chagnes A, Pospiech B (2013) A brief review on hydrometallurgical technologies for recycling spent lithium-ion batteries. *J Chem Technol Biotechnol* 88: 1191–1199.
22. Larcher D, Tarascon JM (2015) Towards greener and more sustainable batteries for electrical energy storage. *Nat Chem* 7: 19–29.
23. Harper G, Sommerville R, Kendrick E, et al. (2019) Recycling lithium-ion batteries from electric vehicles. *Nature* 575: 75–86.
24. Ciez RE, Whitacre JF (2019) Examining different recycling processes for lithium-ion batteries. *Nat Sustainability* 2: 148–156.
25. Sommerville R, Shaw-Stewart J, Goodship V, et al. (2020) A review of physical processes used in the safe recycling of lithium ion batteries. *Sustainable Mater Technol* 25.

26. Zhang T, He Y, Ge L, et al. (2013) Characteristics of wet and dry crushing methods in the recycling process of spent lithium-ion batteries. *J Power Sources* 240: 766–771.
27. Zhang T, He Y, Wang F, et al. (2014) Chemical and process mineralogical characterizations of spent lithium-ion batteries: an approach by multi-analytical techniques. *Waste Manag* 34: 1051–1058.
28. Barik SP, Prabaharan G, Kumar L (2017) Leaching and separation of Co and Mn from electrode materials of spent lithium-ion batteries using hydrochloric acid: Laboratory and pilot scale study. *J Cleaner Prod* 147: 37–43.
29. Diekmann J, Hanisch C, Froböse L, et al. (2016) Ecological Recycling of Lithium-Ion Batteries from Electric Vehicles with Focus on Mechanical Processes. *J Electrochem Soc* 164: A6184–A6191.
30. Yu J, He Y, Ge Z, et al. (2018) A promising physical method for recovery of LiCoO 2 and graphite from spent lithium-ion batteries: Grinding flotation. *Sep Purif Technol* 190: 45–52.
31. Li L, Ge J, Wu F, et al. (2010) Recovery of cobalt and lithium from spent lithium ion batteries using organic citric acid as leachant. *J Hazard Mater* 176: 288–293.
32. Guan J, Li Y, Guo Y, et al. (2016) Mechanochemical Process Enhanced Cobalt and Lithium Recycling from Wasted Lithium-Ion Batteries. *ACS Sustainable Chem Eng* 5: 1026–1032.
33. Silveira AVM, Santana MP, Tanabe EH, et al. (2017) Recovery of valuable materials from spent lithium ion batteries using electrostatic separation. *Int J Miner Process* 169: 91–98.
34. Widijatmoko SD, Fu G, Wang Z, et al. (2020) Recovering lithium cobalt oxide, aluminium, and copper from spent lithium-ion battery via attrition scrubbing. *J Cleaner Prod* 260: 120869.
35. Gratz E, Sa Q, Apelian D, et al. (2014) A closed loop process for recycling spent lithium ion batteries. *J Power Sources* 262: 255–262.
36. Pinegar H, Smith YR (2019) Recycling of End-of-Life Lithium Ion Batteries, Part I: Commercial Processes. *J Sustainable Metall* 5: 402–416.
37. Xue M, Xu Z (2013) Computer simulation of the pneumatic separator in the pneumatic-electrostatic separation system for recycling waste printed circuit boards with electronic components. *Environ Sci Technol* 47: 4598–4604.
38. Huang K, Li J, Xu Z (2011) Enhancement of the recycling of waste Ni-Cd and Ni-MH batteries by mechanical treatment. *Waste Manag* 31: 1292–1299.
39. Zhong X, Liu W, Han J, et al. (2020) Pneumatic separation for crushed spent lithium-ion batteries. *Waste Manag* 118: 331–340.
40. Zhu X, Zhang C, Feng P, et al. (2021) A novel pulsated pneumatic separation with variable-diameter structure and its application in the recycling spent lithium-ion batteries. *Waste Manag* 131: 20–30.
41. Bertuol DA, Toniasso C, Jiménez BM, et al. (2015) Application of spouted bed elutriation in the recycling of lithium ion batteries. *J Power Sources* 275: 627–632.
42. Bi H, Zhu H, Zu L, et al. (2019) A new model of trajectory in eddy current separation for recovering spent lithium iron phosphate batteries. *Waste Manag* 100: 1–9.
43. Marinos D, Mishra B (2015) An Approach to Processing of Lithium-Ion Batteries for the Zero-Waste Recovery of Materials. *J Sustainable Metall* 1: 263–274.

44. Widijatmoko SD, Gu F, Wang Z, et al. (2020) Selective liberation in dry milled spent lithium-ion batteries. *Sustainable Mater Technol* 23: e00134.
45. Peng C, Liu F, Aji AT, et al. (2019) Extraction of Li and Co from industrially produced Li-ion battery waste - Using the reductive power of waste itself. *Waste Manag* 95: 604–611.
46. Vieceli N, Nogueira CA, Guimaraes C, et al. (2018) Hydrometallurgical recycling of lithium-ion batteries by reductive leaching with sodium metabisulphite. *Waste Manag* 71: 350–361.
47. Chen H, Ling M, Hencz L, et al. (2018) Exploring Chemical, Mechanical, and Electrical Functionalities of Binders for Advanced Energy-Storage Devices. *Chem Rev* 118: 8936–8982.
48. He K, Zhang ZY, Alai L, et al. (2019) A green process for exfoliating electrode materials and simultaneously extracting electrolyte from spent lithium-ion batteries. *J Hazard Mater* 375: 43–51.
49. Bottino A, Capannelli G, Munari S, et al. (1988) Solubility parameters of poly (vinylidene fluoride). *J Polym Sci* 26: 785–794.
50. Hanisch C, Haselrieder W, Kwade A (2011) Recovery of Active Materials from Spent Lithium-Ion Electrodes and Electrode Production Rejects. *Glocalized Solutions Sustainability Manuf* 85–89.
51. Song D, Wang X, Zhou E, et al. (2013) Recovery and heat treatment of the Li(Ni1/3Co1/3Mn1/3)O2 cathode scrap material for lithium ion battery. *J Power Sources* 232: 348–352.
52. Song X, Hu T, Liang C, et al. (2017) Direct regeneration of cathode materials from spent lithium iron phosphate batteries using a solid phase sintering method. *RSC Adv* 7: 4783–4790.
53. Bankole OE, Gong C, Lei L (2013) Battery Recycling Technologies: Recycling Waste Lithium Ion Batteries with the Impact on the Environment In-View. *J Environ Ecol* 4: 14–28.
54. He LP, Sun SY, Song XF, et al. (2015) Recovery of cathode materials and Al from spent lithium-ion batteries by ultrasonic cleaning. *Waste Manag* 46: 523–528.
55. Bai Y, Hawley WB, Jafta CJ, et al. (2020) Sustainable recycling of cathode scraps via Cyrene-based separation. *Sustainable Mater Technol* 25: e00202.
56. Zeng X, Li J (2014) Innovative application of ionic liquid to separate Al and cathode materials from spent high-power lithium-ion batteries. *J Hazard Mater* 271: 50–56.
57. Wang M, Tan Q, Liu L, et al. (2019) A low-toxicity and high-efficiency deep eutectic solvent for the separation of aluminum foil and cathode materials from spent lithium-ion batteries. *J Hazard Mater* 380: 120846.
58. Bai Y, Muralidharan N, Li J, et al. (2020) Sustainable Direct Recycling of Lithium‐Ion Batteries via Solvent Recovery of Electrode Materials. *ChemSusChem* 13: 5664–5670.
59. Wang M, Tan Q, Liu L, et al. (2020) Revealing the Dissolution Mechanism of Polyvinylidene Fluoride of Spent Lithium-Ion Batteries in Waste Oil-Based Methyl Ester Solvent. *ACS Sustainable Chem Eng* 8: 7489–7496.
60. Wang H, Liu J, Bai X, et al. (2019) Separation of the cathode materials from the Al foil in spent lithium-ion batteries by cryogenic grinding. *Waste Manag* 91: 89–98.
61. Wang M, Tan Q, Liu L, et al. (2019) Efficient Separation of Aluminum Foil and Cathode Materials from Spent Lithium-Ion Batteries Using a Low-Temperature Molten Salt. *ACS Sustainable Chem Eng* 7: 8287–8294.

62. Ji Y, Jafvert CT, Zhao F (2021) Recovery of cathode materials from spent lithium-ion batteries using eutectic system of lithium compounds. *Resour Conserv Recycl* 170: 105551.
63. Zhang X, Xue Q, Li L, et al. (2016) Sustainable Recycling and Regeneration of Cathode Scraps from Industrial Production of Lithium-Ion Batteries. *ACS Sustainable Chem Eng* 4: 7041–7049.
64. Lee SH, Kim HS, Jin BS (2019) Recycling of Ni-rich Li(Ni0.8Co0.1Mn0.1)O2 cathode materials by a thermomechanical method. *J Alloys Compd* 803: 1032–1036.
65. Nie XJ, Xi XT, Yang Y, et al. (2019) Recycled LiMn2O4 from the spent lithium ion batteries as cathode material for sodium ion batteries: Electrochemical properties, structural evolution and electrode kinetics. *Electrochim Acta* 320: 134626.
66. Ku H, Jung Y, Jo M, et al. (2016) Recycling of spent lithium-ion battery cathode materials by ammoniacal leaching. *J Hazard Mater* 313: 138–146.
67. DeLisio JB, Hu X, Wu T, et al. (2016) Probing the Reaction Mechanism of Aluminum/Poly(vinylidene fluoride) Composites. *J Phys Chem B* 120: 5534–5542.
68. Chen Y, Liu N, Jie Y, et al. (2019) Toxicity Identification and Evolution Mechanism of Thermolysis-Driven Gas Emissions from Cathodes of Spent Lithium-Ion Batteries. *ACS Sustainable Chem Eng* 7: 18228–18235.
69. Wang M, Tan Q, Li J (2018) Unveiling the Role and Mechanism of Mechanochemical Activation on Lithium Cobalt Oxide Powders from Spent Lithium-Ion Batteries. *Environ Sci Technol* 52: 13136–13143.
70. Nan J, Han D, Zuo X (2005) Recovery of metal values from spent lithium-ion batteries with chemical deposition and solvent extraction. *J Power Sources* 152: 278–284.
71. Zhan R, Yang Z, Bloom I, et al. (2020) Significance of a Solid Electrolyte Interphase on Separation of Anode and Cathode Materials from Spent Li-Ion Batteries by Froth Flotation. *ACS Sustainable Chem Eng* 9: 531–540.
72. Zhan R, Oldenburg Z, Pan L (2018) Recovery of active cathode materials from lithium-ion batteries using froth flotation. *Sustainable Mater Technol* 17: e00062.
73. Nie H, Xu L, Song D, et al. (2015) LiCoO2: recycling from spent batteries and regeneration with solid state synthesis. *Green Chemistr* 17: 1276–1280.
74. Xiao J, Li J, Xu Z (2017) Novel Approach for in Situ Recovery of Lithium Carbonate from Spent Lithium Ion Batteries Using Vacuum Metallurgy. *Environ Sci Technol* 51: 11960–11966.
75. Hanisch C, Loellhoeffel T, Diekmann J, et al. (2015) Recycling of lithium-ion batteries: a novel method to separate coating and foil of electrodes. *J Cleaner Prod* 108: 301–311.
76. Zhang G, He Y, Wang H, et al. (2020) Removal of Organics by Pyrolysis for Enhancing Liberation and Flotation Behavior of Electrode Materials Derived from Spent Lithium-Ion Batteries. *ACS Sustainable Chem Eng* 8: 2205–2214.
77. Zhan R, Payne T, Leftwich T, et al. (2020) De-agglomeration of cathode composites for direct recycling of Li-ion batteries. *Waste Manag* 105: 39–48.
78. Kuo CY, Lin HN, Tsai HA, et al. (2008) Fabrication of a high hydrophobic PVDF membrane via nonsolvent induced phase separation. *Desalination* 233: 40–47.
79. Zhang G, Du Z, He Y, et al. (2019) A Sustainable Process for the Recovery of Anode and Cathode Materials Derived from Spent Lithium-Ion Batteries. *Sustainability* 11: 2363.

80. He Y, Zhang T, Wang F, et al. (2017) Recovery of LiCoO2 and graphite from spent lithium-ion batteries by Fenton reagent-assisted flotation. *J Cleaner Prod* 143: 319–325.
81. Holtstiege F, Wilken A, Winter M, et al. (2017) Running out of lithium? A route to differentiate between capacity losses and active lithium losses in lithium-ion batteries. *Phys Chem Chem Phys* 19: 25905–25918.
82. Matsumura Y, Wang S, Mondori J (1995) Mechanism leading to irreversible capacity loss in Li ion rechargeable batteries. *J Electrochem Soc* 142: 2914–2918.
83. Sun Y, Lee HW, Seh ZW, et al. (2016) High-capacity battery cathode prelithiation to offset initial lithium loss. *Nat Energy* 1: 15008.
84. Zhou H, Xin F, Pei B, et al. (2019) What Limits the Capacity of Layered Oxide Cathodes in Lithium Batteries? *ACS Energy Lett* 4: 1902–1906.
85. Li T, Yuan XZ, Zhang L, et al. (2019) Degradation Mechanisms and Mitigation Strategies of Nickel-Rich NMC-Based Lithium-Ion Batteries. *Electrochem Energy Rev* 3: 43–80.
86. Lou S, Shen B, Zuo P, et al. (2015) Electrochemical performance degeneration mechanism of LiCoO2 with high state of charge during long-term charge/discharge cycling. *RSC Adv* 5: 81235–81242.
87. Zhao Y, Yuan X, Jiang L, et al. (2020) Regeneration and reutilization of cathode materials from spent lithium-ion batteries. *Chem Eng J* 383: 123089.
88. Shi Y, Chen G, Chen Z (2018) Effective regeneration of LiCoO2 from spent lithium-ion batteries: a direct approach towards high-performance active particles. *Green Chem* 20: 851–862.
89. Shi Y, Chen G, Liu F, et al. (2018) Resolving the Compositional and Structural Defects of Degraded LiNixCoyMnzO2 Particles to Directly Regenerate High-Performance Lithium-Ion Battery Cathodes. *ACS Energy Lett* 3: 1683–1692.
90. Meng X, Hao J, Cao H, et al. (2019) Recycling of LiNi1/3Co1/3Mn1/3O2 cathode materials from spent lithium-ion batteries using mechanochemical activation and solid-state sintering. *Waste Manag* 84: 54–63.
91. Li X, Zhang J, Song D, et al. (2017) Direct regeneration of recycled cathode material mixture from scrapped LiFePO4 batteries. *J Power Sources* 345: 78–84.
92. Shi Y, Zhang M, Meng YS, et al. (2019) Ambient-Pressure Relithiation of Degraded LixNi0.5Co0.2Mn0.3O2($0 < x < 1$) via Eutectic Solutions for Direct Regeneration of Lithium-Ion Battery Cathodes. *Adv Energy Mater* 9: 1900454.
93. Wang H, Whitacre JF (2018) Direct Recycling of Aged LiMn2O4 Cathode Materials used in Aqueous Lithium-ion Batteries: Processes and Sensitivities. *Energy Technol* 6: 2429–2437.
94. Antolini E (2004) LiCoO2: formation, structure, lithium and oxygen nonstoichiometry, electrochemical behaviour and transport properties. *Solid State Ionics* 170: 159–171.
95. Dahn JR, Fuller EW, Obrovac M, et al. (1994) Thermal stability of LixCoO2, LixNiO2 and λ-MnO2 and consequences for the safety of Li-ion cells. *Solid State Ionics* 69: 265–270.
96. Lundblad A, Bergman B (1997) Synthesis of LiCoO2 starting from carbonate precursors II. Influence of calcination conditions and leaching. *Solid State Ionics* 96: 183–193.
97. Chang ZR, Yu X, Tang HW, et al. (2011) Synthesis of LiNi1/3Co1/3Al1/3O2 cathode material with eutectic molten salt LiOH-LiNO3. *Powder Technol* 207: 396–400.

98. Zhang Z, He W, Li G, et al. (2013) Renovation of LiCoO2 crystal structure from spent lithium ion batteries by ultrasonic hydrothermal reaction. *Res Chem Intermed* 41: 3367–3373.
99. Zhu S (2016) Renovation of Lithium Cobalt Oxide from Spent Lithium Ion Batteries by an Aqueous Pulsed Discharge Plasma. *Int J Electrochem Sci* 6403–6411.
100. Gao H, Yan Q, Xu P, et al. (2020) Efficient Direct Recycling of Degraded LiMn2O4 Cathodes by One-Step Hydrothermal Relithiation. *ACS Appl Mater Interfaces* 12: 51546–51554.
101. Wang T, Luo H, Bai Y, et al. (2020) Direct Recycling of Spent NCM Cathodes through Ionothermal Lithiation. *Adv Energy Mater* 10: 2001204.
102. Zhang L, Xu Z, He Z (2020) Electrochemical Relithiation for Direct Regeneration of LiCoO2 Materials from Spent Lithium-Ion Battery Electrodes. *ACS Sustainable Chem Eng* 8: 11596–11605.
103. Matis WJL, Yonemoto BT, YIN Y, et al. (2019) Method for recycling and refreshing cathode material, refreshed cathode material and lithium ion battery.
104. Argonne National Laboratory (2018) EverBatt. Available from: https://www.anl.gov/egs/everbatt.
105. The National Renewable Energy Laboratory (2021) Battery Second-Use Repurposing Cost Calculator. Available from: https://www.nrel.gov/transportation/b2u-calculator.html.

AIMS Press